Materials Transactions, Vol. 49, No. 2 (2008) pp. 294 to 303

Numerical Analysis for Kinetics of Reactive Diffusion Controlled by Boundary and Volume Diffusion in a Hypothetical Binary System

Akira Furuto[1] and Masanori Kajihara[2,*]

[1]*Graduate School, Tokyo Institute of Technology, Yokohama 226-8502, Japan*
[2]*Department of Materials Science and Engineering, Tokyo Institute of Technology, Yokohama 226-8502, Japan*

A hypothetical binary system composed of one intermetallic compound and two primary solid-solution phases has been considered in order to examine the kinetics of the reactive diffusion controlled by boundary and volume diffusion. If a semi-infinite diffusion couple initially consisting of the two primary solid-solution phases with solubility compositions is isothermally annealed at an appropriate temperature, the compound layer will be surely produced at the interface between the primary solid-solution phases. In the primary solid-solution phases, however, there is no diffusional flux. Furthermore, we suppose that the compound layer is composed of a single layer of square-rectangular grains with an identical dimension. Here, the square basal-plane is parallel to the interface, and hence the height is equal to the thickness of the compound layer. Under such conditions, the growth behavior of the compound layer has been analyzed numerically. In order to simplify the analysis, the following assumptions have been adopted for the compound layer: there is no grain boundary segregation; and volume and boundary diffusion takes place along the direction perpendicular to the interface. When the size of the basal-plane remains constant independently of the annealing time, the thickness of the compound layer is proportional to the square root of the annealing time. In contrast, the growth of the compound layer takes place in complicated manners, if the size of the basal-plane increases in proportion to a power function of the annealing time. Nevertheless, around a certain critical annealing time, the thickness of the compound layer is approximately expressed as a power function of the annealing time. For each grain, the layer growth is associated with increase in the height, and the grain growth is relevant to increase in the size of the basal-plane. The exponent for the layer growth almost linearly decreases with increasing exponent for the grain growth. [doi:10.2320/matertrans.MRA2007192]

(Received August 6, 2007; Accepted November 12, 2007; Published December 27, 2007)

Keywords: *diffusion, kinetics, modeling*

1. Introduction

The growth behavior of intermetallic compounds during reactive diffusion has been experimentally observed for various alloy systems by many investigators.[1–27] In such an experiment, a semi-infinite diffusion couple consisting of different pure metals or alloys may be isothermally annealed at an appropriate temperature. Owing to annealing, some of the stable compounds will be formed as layers at the interface in the diffusion couple. If the growth of the compound layers is controlled by volume diffusion, a parabolic relationship holds good between the total thickness of the compound layers and the annealing time. Here, the parabolic relationship means that the total thickness is proportional to the square root of the annealing time. However, volume diffusion is not necessarily the rate-controlling process of reactive diffusion for all the alloy systems.

The kinetics of the reactive diffusion in the binary Au-Sn system was experimentally observed using Sn/Au/Sn diffusion couples at solid-state temperatures in previous studies.[28–31] In those experiments, the diffusion couples were isothermally annealed at temperatures between $T =$ 393 and 473 K for various times in an oil bath with silicone oil. Here, T is the annealing temperature. Due to annealing, compound layers of AuSn, $AuSn_2$ and $AuSn_4$ are produced at the Au/Sn interface in the diffusion couple. According to the observation, the total thickness of the Au-Sn compound layers is mathematically expressed as a power function of the annealing time, and the exponent of the power function is 0.48, 0.42, 0.39 and 0.36 at $T = 393$, 433, 453 and 473 K, respectively. Such temperature dependence of the exponent indicates that boundary diffusion as well as volume diffusion contributes to the rate-controlling process and grain growth occurs in the compound layers at certain rates at higher annealing temperatures.[30] As the annealing temperature decreases, the contribution of the boundary diffusion becomes more remarkable, but the grain growth slows down. This is the reason why the exponent is smaller than 0.5 at higher annealing temperatures but close to 0.5 at lower annealing temperatures. The reactive diffusion controlled by boundary and volume diffusion takes place in many alloy systems.[28–45] The rate-controlling process of such reactive diffusion is hereafter called the mixed rate-controlling process.

The kinetics of the mixed rate-controlling process was theoretically analyzed using a mathematical model by Farrell and Glimer.[34] In their model, a polycrystalline compound layer consisting of tabular grains with an identical width and flat grain boundaries with a certain thickness is formed at the interface between solid-solution phases with solubility compositions in a semi-infinite diffusion couple. Here, each tabular grain is sandwiched between the parallel grain boundaries perpendicular to the interface. During growth of the compound layer, one-dimensional boundary diffusion takes place along the grain boundary, and two-dimensional volume diffusion occurs along the directions perpendicular to the grain boundary and the interface. However, no diffusional flux exists in the solid-solution phases. Under such conditions, the growth behavior of the compound layer was calculated numerically. The numerical calculation was carried out mainly for the growth of the compound layer without grain growth. According to the calculation, the thickness of the compound layer increases in proportion to a power function of the annealing time, and the exponent of the

*Corresponding author, E-mail: kajihara@materia.titech.ac.jp

power function takes a constant value of 0.48. Thus, the exponent is slightly smaller than 0.5. In order for the compound layer to grow continuously, solute atoms should be transported along the grain boundary over long distances. However, the solute atoms in the grain boundary will be partially wasted due to the volume diffusion along the direction perpendicular to the grain boundary. Such partial wastage of the solute atoms slightly decelerates the growth of the compound layer. This is the reason why the exponent is slightly smaller than 0.5.

The growth of a compound layer controlled by boundary diffusion was theoretically analyzed using a different model by Corcoran *et al.*[35] In their model of a semi-infinite diffusion couple, a polycrystalline compound layer is composed of cylindrical grains with an identical diameter, where the rotation axis of the grain is perpendicular to the interface and the diameter of the grain is expressed as a power function of the annealing time. Unlike the model by Farrell and Glimer,[34] only boundary diffusion takes place in the compound layer, but volume diffusion occurs merely in the neighboring phase ahead of the growing compound layer. If the contribution is much greater for the boundary diffusion than for the volume diffusion, the thickness of the compound layer is proportional to a power function of the annealing time.[35] Furthermore, the exponent of the power function is much smaller than 0.5 on condition that grain growth considerably occurs in the compound layer. Such conclusions may be drawn also for the mixed rate-controlling process with grain growth. Unfortunately, however, reliable information of the kinetics is not available for this type of mixed rate-controlling process. In order to examine the influence of grain growth on the kinetics of the mixed rate-controlling process, the growth behavior of a polycrystalline compound layer in a semi-infinite diffusion couple initially composed of solid-solution phases has been numerically analyzed in the present study. Here, the compound layer consists of a single layer of square-rectangular grains with an identical size, and volume and boundary diffusion occurs across the compound layer. However, it is assumed that there is no diffusional flux in the solid-solution phases. This assumption emphasizes the influence. The kinetics has been quantitatively discussed on the basis of the numerical analysis.

2. Model

Let us consider a hypothetical binary A-B system composed of two primary solid-solution phases and one intermetallic compound. Hereafter, the A-rich and B-rich solid-solution phases are called the α and γ phases, respectively, and the intermetallic compound is designated the β phase. For such a binary system, we consider a semi-infinite diffusion couple consisting of the α and γ phases with initial compositions of $c^{\alpha\beta}$ and $c^{\gamma\beta}$, respectively. Here, c is the concentration of component B measured in mol per unit volume, and $c^{\alpha\beta}$ and $c^{\gamma\beta}$ correspond to the composition of the α phase for the α/β tie-line and that of the γ phase for the β/γ tie-line, respectively, in the phase diagram of the binary A-B system. The semi-infinite diffusion couple means that the thicknesses of the α and γ phases are semi-infinite and the α/γ interface is flat. In such a diffusion couple, the interdiffusion of components A and B occurs unidirectionally along the direction perpendicular to the flat interface. This direction is hereafter called the diffusional direction. When the diffusion couple is isothermally annealed at temperature T for an appropriate time, the β phase will be produced at the interface owing to the reactive diffusion between the α and γ phases. Here, T is high enough for the reactive diffusion to occur sufficiently fast but lower than the temperature at which the liquid phase is stable. The concentration profile of component B across the β phase along the diffusional direction is drawn in Fig. 1. In this figure, the ordinate shows the composition c, and the abscissa indicates the distance x measured from the initial position of the α/γ interface. Dashed lines and solid curves show the concentration profiles before and after annealing, respectively, and $z^{\alpha\beta}$ and $z^{\beta\gamma}$ indicate the positions of the α/β and β/γ interfaces, respectively, after annealing. If the local equilibrium is realized at each migrating interface during annealing, the compositions of the neighboring phases at the interface coincide with those of the corresponding tie-line at temperature T. Such a reaction will actually proceed on condition that the interface diffusion across the migrating interface is much faster than the interdiffusion across the compound layer. In this case, the migration of the interface is controlled by the interdiffusion. This type of reaction is usually denominated the diffusion-controlling reaction. For the diffusion-controlling reaction, the migration rates $dz^{\alpha\beta}/dt$ and $dz^{\beta\gamma}/dt$ of the α/β and β/γ interfaces, respectively, are related to the flux balance at the interface by the equations[46]

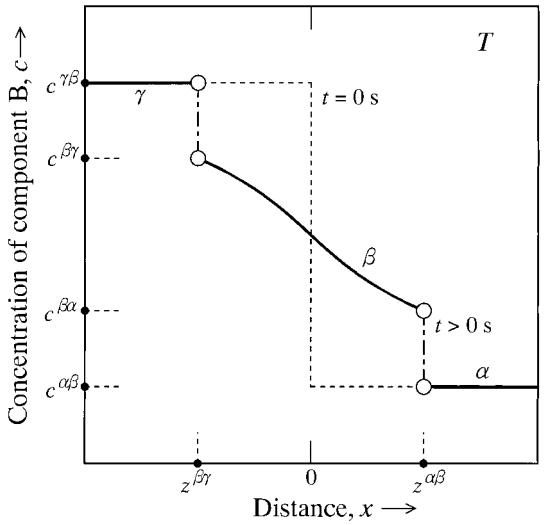

Fig. 1 Concentration profile of component B across the β phase in the semi-infinite diffusion couple along the diffusional direction.

$$(c^{\beta\alpha} - c^{\alpha\beta})\frac{dz^{\alpha\beta}}{dt} = J^{\beta\alpha} \tag{1a}$$

and

$$(c^{\gamma\beta} - c^{\beta\gamma})\frac{dz^{\beta\gamma}}{dt} = -J^{\beta\gamma}, \tag{1b}$$

respectively. Here, $J^{\beta\alpha}$ and $J^{\beta\gamma}$ are the diffusional fluxes of component B in the β phase at the α/β and β/γ interfaces, respectively. According to Fick's first law, the diffusional

fluxes $J^{\beta\alpha}$ and $J^{\beta\gamma}$ are proportional to the concentration gradients $(\partial c^{\beta}/\partial x)_{x=z^{\alpha\beta}}$ and $(\partial c^{\beta}/\partial x)_{x=z^{\beta\gamma}}$ in the β phase at the α/β and β/γ interfaces, respectively, as follows:

$$J^{\beta\alpha} = -D\left(\frac{\partial c^{\beta}}{\partial x}\right)_{x=z^{\alpha\beta}} \tag{2a}$$

and

$$J^{\beta\gamma} = -D\left(\frac{\partial c^{\beta}}{\partial x}\right)_{x=z^{\beta\gamma}}. \tag{2b}$$

In eq. (2), D is the diffusion coefficient for the interdiffusion across the β phase. Since there is no concentration gradient in the α and γ phases, no diffusional flux exists in these phases. If the diffusion coefficient D is independent of the composition c^{β} of the β phase, Fick's second law is expressed as

$$\frac{\partial c^{\beta}}{\partial t} = D\frac{\partial^2 c^{\beta}}{\partial x^2} \tag{3}$$

for the β phase. Equation (3) shows that the composition c^{β} is a function of the distance x and the annealing time t. For the semi-infinite diffusion couple, the initial conditions are described as

$$c^{\alpha}(x > 0, t = 0) = c^{\alpha\beta} \tag{4a}$$

and

$$c^{\gamma}(x < 0, t = 0) = c^{\gamma\beta}, \tag{4b}$$

and the boundary conditions are expressed by the equations

$$c^{\alpha}(x \geq z^{\alpha\beta}, t > 0) = c^{\alpha\beta}, \tag{5a}$$

$$c^{\beta}(x = z^{\alpha\beta}, t > 0) = c^{\beta\alpha}, \tag{5b}$$

$$c^{\beta}(x = z^{\beta\gamma}, t > 0) = c^{\beta\gamma} \tag{5c}$$

and

$$c^{\gamma}(x \leq z^{\beta\gamma}, t > 0) = c^{\gamma\beta}. \tag{5d}$$

When the diffusion coefficient D is constant independent of annealing time t at a given temperature of T, eqs. (1)–(3) are analytically solved under the initial and boundary conditions of eqs. (4) and (5).[46,47] However, no analytical solution is known, if D varies depending on t. In such a case, eqs. (1)–(3) should be solved numerically.

For the numerical calculation, Crank-Nicolson implicit method[48] was combined with a finite-difference technique.[49] In the finite-difference technique, the distance x and the annealing time t are divided into intervals Δx and Δt, respectively, and then described as $x_i = i\Delta x$ and $t_j = j\Delta t$, respectively. Here, i and j are the dimensionless integers that are equal to or greater than 0. The concentration profile of component B in the β phase at $t = t_j$ is schematically shown in Fig. 2. In this figure, the ordinate and the abscissa indicate the composition c and the distance x, respectively. Unlike Fig. 1, however, the distance x is measured from the β/γ interface in Fig. 2. Hereafter, the origin of the distance x is defined in this manner. Furthermore, z is the position of the α/β interface measured from the origin of the distance x, and thus equivalent to the thickness of the β phase. Thus, there exists the following relationship among $z^{\alpha\beta}$, $z^{\beta\gamma}$ and z.

$$z = z^{\alpha\beta} - z^{\beta\gamma} \tag{6}$$

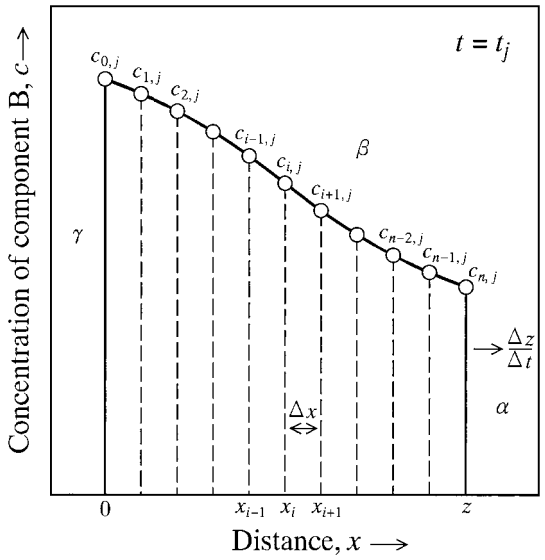

Fig. 2 Concentration profile of component B in the β phase of the semi-infinite diffusion couple along the diffusional direction.

In Fig. 2, the thickness z is divided into grid points with a number of $n + 1$. The interval Δx between the neighboring grid points is obtained by the relationship $\Delta x = z/n$. Hence, $z = n\Delta x = x_n$. The composition of the β phase with $x = x_i$ and $t = t_j$ is denoted by $c_{i,j}$. Since z is a function of t, Δx also varies depending on t. In contrast, Δt is kept constant independently of t. The compositions $c_{0,j}$ and $c_{n,j}$ correspond to the values at the β/γ and α/β interfaces, respectively. During annealing, $c_{i,j}$ changes depending on t for $0 < i < n$, but takes constant values of $c_{0,0}$ or $c^{\beta\gamma}$ and $c_{n,0}$ or $c^{\beta\alpha}$ for $i = 0$ and n, respectively. Consequently, we obtain

$$\begin{aligned} &-rc_{i-1,j+1} + 2(1+r)c_{i,j+1} - rc_{i+1,j+1} \\ &= (r - p_i v_j)c_{i-1,j} + 2(1-r)c_{i,j} + (r + p_i v_j)c_{i+1,j} \end{aligned} \tag{7a}$$

for $1 < i < n - 1$,

$$\begin{aligned} &2(1+r)c_{1,j+1} - rc_{2,j+1} \\ &= (2r - p_i v_j)c_{0,0} + 2(1-r)c_{1,j} + (r + p_i v_j)c_{2,j} \end{aligned} \tag{7b}$$

for $i = 1$, and

$$\begin{aligned} &-rc_{n-2,j+1} + 2(1+r)c_{n-1,j+1} \\ &= (r - p_i v_j)c_{n-2,j} + 2(1-r)c_{n-1,j} + (2r + p_i v_j)c_{n,0} \end{aligned} \tag{7c}$$

for $i = n - 1$. Here, r and p_i are defined as

$$r = \frac{D(t_j)\Delta t}{\Delta x^2} \tag{8a}$$

and

$$p_i = \frac{i\Delta t}{2z_{j+1}}, \tag{8b}$$

respectively. The notation $D(t_j)$ explicitly indicates that D varies depending on t_j. The migration rate v_j of the α/β interface measured from the β/γ interface at $t = t_j$ is obtained as

$$\begin{aligned} v_j = \frac{\Delta z_j}{\Delta t} = \frac{z_{j+1} - z_j}{\Delta t} &= q^{\beta\gamma}(c_{2,j} - 4c_{1,j} + 3c_{0,0}) \\ &- q^{\alpha\beta}(c_{n-2,j} - 4c_{n-1,j} + 3c_{n,0}), \end{aligned} \tag{9}$$

where $q^{\alpha\beta}$ and $q^{\beta\gamma}$ are defined as

$$q^{\alpha\beta} = \frac{D(t_j)}{2(c^{\beta\alpha} - c^{\alpha\beta})\Delta x} \tag{10a}$$

and

$$q^{\beta\gamma} = \frac{D(t_j)}{2(c^{\gamma\beta} - c^{\beta\gamma})\Delta x}, \tag{10b}$$

respectively. In eqs. (8b) and (9), z_j and z_{j+1} are the positions of the α/β interface at $t = t_j$ and t_{j+1}, respectively. Equation (7) is simply expressed using matrices $\boldsymbol{A}$, $\boldsymbol{B}$ and $\boldsymbol{C}$ as follows.

$$\boldsymbol{AC} = \boldsymbol{B} \tag{11}$$

Here,

$$\boldsymbol{A} = \begin{pmatrix} 2(1+r) & -r & 0 & \dots & 0 & 0 \\ -r & 2(1+r) & -r & \dots & 0 & 0 \\ 0 & -r & 2(1+r) & \dots & 0 & 0 \\ \vdots & \vdots & \vdots & \ddots & \vdots & \vdots \\ 0 & 0 & 0 & -r & 2(1+r) & -r \\ 0 & 0 & 0 & 0 & -r & 2(1+r) \end{pmatrix}, \tag{12a}$$

$$\boldsymbol{B} = \begin{pmatrix} (2r - p_1 v_j)c_{0,0} + 2(1-r)c_{1,j} + (r + p_1 v_j)c_{2,j} \\ (r - p_2 v_j)c_{1,j} + 2(1-r)c_{2,j} + (r + p_2 v_j)c_{3,j} \\ (r - p_3 v_j)c_{2,j} + 2(1-r)c_{3,j} + (r + p_3 v_j)c_{4,j} \\ \vdots \\ (r - p_{n-2} v_j)c_{n-3,j} + 2(1-r)c_{n-2,j} + (r + p_{n-2} v_j)c_{n-1,j} \\ (r - p_{n-1} v_j)c_{n-2,j} + 2(1-r)c_{n-1,j} + (2r + p_{n-1} v_j)c_{n,0} \end{pmatrix} \tag{12b}$$

and

$$\boldsymbol{C} = \begin{pmatrix} c_{1,j+1} \\ c_{2,j+1} \\ c_{3,j+1} \\ \vdots \\ c_{n-2,j+1} \\ c_{n-1,j+1} \end{pmatrix}. \tag{12c}$$

The matrix $\boldsymbol{C}$ composed of the unknown composition $c_{i,j+1}$ is calculated for the matrix $\boldsymbol{B}$ containing the known composition $c_{i,j}$ from eq. (11). Since the matrix $\boldsymbol{A}$ is tridiagonal as shown in eq. (12a), the calculation can be readily carried out by an appropriate linear algebra technique even for a large number of n.[50)]

3. Results and Discussion

3.1 Growth behavior of β phase

In the present model, no diffusional flux exists in the α and γ phases of the semi-infinite diffusion couple. In such a case, the growth of the β phase is governed by the interdiffusion across the β phase. Hence, the influence of grain growth on the kinetics of the mixed rate-controlling process is suitably emphasized in the present model. As mentioned earlier, the β phase is formed as a layer in the semi-infinite diffusion couple. Hereafter, the layer of the β phase is merely called the β layer.

When the β layer grows according to the mixed rate-controlling process and grain growth occurs in the β layer, the diffusion coefficient D monotonically decreases with increasing annealing time t due to the grain growth. In order to express the diffusion coefficient $D(t)$ as a mathematical function of the annealing time t, we assume that the β layer is composed of a single layer of square-rectangular grains with an identical dimension. Such a square-rectangular grain is schematically shown in Fig. 3. In this figure, d is the side length of the square basal-plane, z is the height, and δ is the thickness of the grain boundaries surrounding the grain. Here, the z axis is perpendicular to the interface, and hence the basal-plane is parallel to the interface. Consequently, the height of the square-rectangular grain is equivalent to the thickness of the β layer. On the other hand, the side length d stands for the grain size of the square-rectangular grain. In this case, the fraction f of the total cross-sectional area for the grain boundaries to the whole cross-sectional area of the β layer is evaluated by the following equation.

$$f = \frac{2\delta}{d} \tag{13}$$

In order to simplify the analysis, the following assumptions were adopted for the β layer: (A) there is no grain boundary segregation; (B) volume and boundary diffusion takes place along the z axis; and (C) grain growth starts to occur at a certain annealing time of t_s. Due to assumptions A and B, the effective diffusion coefficient D across the β layer is readily calculated by the equation

$$D = (1 - f)D^{v} + fD^{b}, \tag{14}$$

where D^{v} is the diffusion coefficient of the volume diffusion, and D^{b} is that of the boundary diffusion. Furthermore, according to assumption C, the grain size d is expressed as a power function of the annealing time t by the following equation.

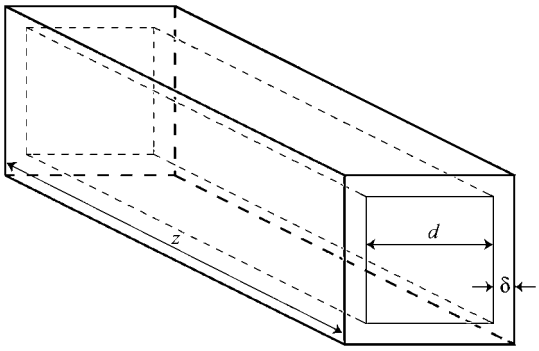

Fig. 3 Schematic drawing of square-rectangular grain in the β phase.

$$d = d_s + k_d\left(\frac{t_d}{t_0}\right)^p \tag{15}$$

Here, d_s is the value of d at $t \leq t_s$, k_d is the proportionality coefficient, p is the exponent, $t_d = t - t_s$, and t_0 is unit time, 1 s. The proportionality coefficient k_d possesses the same dimension as d, but the exponent p is dimensionless. From eqs. (13)–(15), D is finally expressed as an explicit function of t. Combining eqs. (13)–(15) with eqs. (8)–(12), the growth behavior of the β layer was calculated numerically. In the present analysis, the following parameters were used for the whole numerical calculation: $y^{\alpha\beta} = 0.1$, $y^{\beta\alpha} = 0.3$, $y^{\beta\gamma} = 0.7$, $y^{\gamma\beta} = 0.9$, $\delta = 5 \times 10^{-10}$ m and $d_s = 10^{-6}$ m. Here, y is the mol fraction of component B. Furthermore, t_s is defined as the annealing time t where z reaches to d_s. Hence, $z < d = d_s$ at $t < t_s$, but $z = d = d_s$ at $t = t_s$. This means that the square-rectangular grain becomes the cubic grain with a side length of d_s at $t = t_s$. At $t > t_s$, however, d becomes surely greater than d_s, but greater or smaller than z depending on k_d and p. In Figs. 1 and 2, the composition is indicated with the concentration c of component B measured in mol per unit volume. On the other hand, the mol fraction y is practically used to express the composition of each phase. However, the mol fraction y is readily converted into the concentration c by the equation $c = y/V_m$, where V_m is the molar volume of the relevant phase. If the molar volume V_m is assumed to be constant independent of the composition, the concentration $c_{i,j}$ in eqs. (9)–(12) is automatically replaced with the mol fraction $y_{i,j}$. Here, the subscripts i and j of the mol fraction y possess the same meanings as the concentration c. As previously mentioned, at $t \leq t_s$, the grain growth does not occur and thus $d = d_s$. Therefore, D is constant independent of t according to eqs. (13)–(15). In such a case, z_j and $y_{i,j}$ are calculated analytically.[46,47] The analytical values of z_j and $y_{i,j}$ at $t_j = t_s$ were used as the initial values for the numerical calculation of the new values at $t_{j+1} = t_j + \Delta t$. The accuracy of the numerical calculation increases with decreasing values of Δx and Δt. However, very small values of Δx and Δt result in an extremely long computing time. Thus, there is an optimum combination of Δx and Δt depending on the power of a computer. In the present analysis, a constant value of $\Delta t = 0.1$ s was adopted for the numerical calculation up to $t_{j+1} = 10^7$ s. On the other hand, appropriate values of n and Δx were determined from eq. (8a) and the equation $\Delta x = z/n$ during iteration in order to satisfy $r < 0.5$.

Typical results for the numerical calculation are shown as solid curves in Fig. 4. In this figure, the following parameters were used for the calculation: $D^v = 10^{-15}$ m^2/s, $D^b = 10^{-10}$ m^2/s, $t_s = 6.4$ s, $k_d = 10^{-7}$ m and $p = 0$–0.6. In contrast, a dashed line indicates the result for the volume-diffusion controlling process with $D = D^v$. In Fig. 4, the ordinate shows the logarithm of the thickness z of the β layer, and the abscissa indicates the logarithm of the annealing time t. As can be seen, the thickness z monotonically increases with increasing annealing time t in different manners depending on the exponent p. For $p = 0$, the grain growth does not occur, and hence the fraction f remains constant during growth of the β layer. Therefore, D is constant independent of t. In such a case, the solid curve becomes straight, and hence z is expressed as a power function of t by the equation

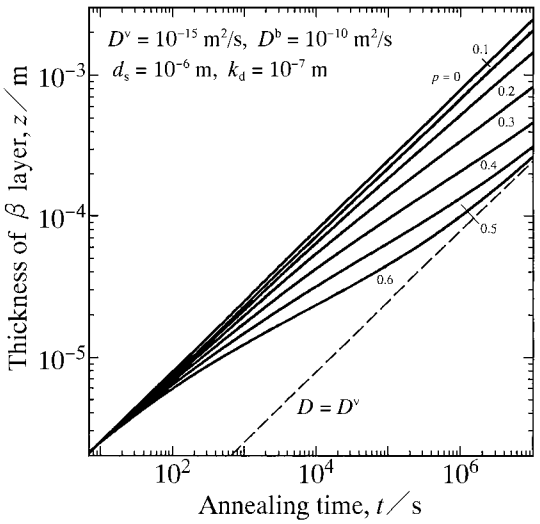

Fig. 4 The thickness z of the β layer versus the annealing time t calculated for $D^v = 10^{-15}$ m^2/s, $D^b = 10^{-10}$ m^2/s, $k_d = 10^{-7}$ m and $p = 0$–0.6. A dashed line shows the calculation for $D = D^v$.

$$z = k\left(\frac{t}{t_0}\right)^q, \tag{16}$$

where k and q are the proportionality coefficient and the exponent, respectively. For the straight solid line with $p = 0$ in Fig. 4, $k = 7.88 \times 10^{-7}$ m and $q = 0.5$ are obtained from eq. (16). On the other hand, the dashed line provides $k = 7.84 \times 10^{-8}$ m and $q = 0.5$. Thus, the parabolic relationship holds good not only for the volume-diffusion controlling process but also for the mixed rate-controlling process without grain growth. However, k is one order of magnitude greater for the latter rate-controlling process than for the former rate-controlling process. Thus, the growth of the β layer is accelerated by the boundary diffusion, though the parabolic relationship holds good in both rate-controlling processes.

Since $d = d_s$ at $t \leq t_s$, the solid curves for $p > 0$ coincide with the solid line for $p = 0$ at $t \leq t_s$. As the annealing time t increases at $t > t_s$, however, the solid curves gradually deviate from the solid line, and then asymptotically approach to the dashed line. The rate of the approach to the dashed line increases with increasing value of p at a constant value of k_d. For such solid curves, z cannot be expressed as a power function of t with a constant value of q. The dependence of q on t was evaluated from the following equation using z_j and

z_{j+1} at $t = t_j$ and t_{j+1}, respectively.

$$q = \frac{\ln(z_{j+1}/z_j)}{\ln(t_{j+1}/t_j)} \tag{17}$$

The evaluation was carried out for the solid curves in Fig. 4. The results for $p = 0.1$–0.6 are shown as solid curves in Fig. 5(a)–(f), respectively. The evaluation was executed further for $k_d = 2 \times 10^{-7}$–6×10^{-7} m as well as $k_d = 1 \times 10^{-7}$ m. The corresponding results for $p = 0.1$–0.6 are also indicated as solid curves in Fig. 5(a)–(f), respectively. In this figure, the ordinate shows q, and the abscissa indicates the logarithm of t. For $p = 0.1$ in Fig. 5(a), q attains to maximum values at annealing times around $t = 10^3$ s. In contrast, q monotonically decreases with increasing value of k_d. Nevertheless, q is rather close to 0.5 at $t = 10^2$–10^7 s. Although a similar tendency is recognized also for $p = 0.2$ in Fig. 5(b), q is slightly smaller for $p = 0.2$ than for $p = 0.1$. On the other hand, for $p = 0.3$ in Fig. 5(c), q varies depending on t in complicated manners. Nonetheless, q reaches to an almost constant plateau value of $q_c = 0.38$ at a certain annealing time of $t = t_c$. Here, the term "plateau" means that q is rather insensitive to t at annealing times around $t = t_c$. Thus, eq. (16) approximately holds good at the plateau stage. The critical annealing time t_c for the plateau value $q = q_c$ monotonically decreases with increasing value of k_d. According to the results in Fig. 5(d)–(f), $q_c = 0.34$, 0.30 and 0.27 for $p = 0.4$, 0.5 and 0.6, respectively. Furthermore, the solid curve for $k_d = 6 \times 10^{-7}$ m in Fig. 5(b) gives $q_c = 0.42$ for $p = 0.2$, and the solid line in Fig. 4 provides $q_c = 0.5$ for $p = 0$. These values of q_c are plotted as open circles against the exponent p in Fig. 6. As can be seen, q_c monotonically decreases from 0.5 to 0.27 with increasing value of p from 0 to 0.6. Consequently, the exponent q_c becomes much smaller than 0.5 on condition that the grain growth occurs considerably in the β layer. A solid curve passing through the open circles is slightly convex downwards at $p > 0.4$, but almost straight at $p < 0.4$. Thus, there exists an approximately linear relationship between q_c and p at $p < 0.4$.

The results for $p = 0.4$–0.6 in Fig. 5(d)–(f) are shown again as solid curves in Fig. 7(a)–(c), respectively. However, only the results of $k_d = 1 \times 10^{-7}$–3×10^{-7} m indicating rather clear plateau stages are represented in Fig. 7. In this figure, the ordinate on the left-hand side indicates q, and the abscissa shows the logarithm of t. As the annealing time t increases, q gradually decreases at $t < t_c$, and then reaches to q_c at $t = t_c$. On the other hand, at $t > t_c$, q monotonically increases with increasing annealing time t. Unlike Fig. 5(c)–(f), however, t_c is longer than 10^7 s for most of the solid curves in Fig. 5(a) and (b). Hence, q_c cannot appear on these solid curves. Such annealing time dependence of q is attributed to variation in the contribution of the boundary diffusion to the effective diffusion in the β layer. In order to examine such variation, the ratio R is defined as

$$R = \frac{fD^b}{D}. \tag{18}$$

From eq. (18), R was calculated as a function of t. The results for the solid curves are shown as dashed curves in Fig. 7. In this figure, the ordinate on the right-hand side indicates R. Furthermore, R_c and q_c are shown as open circles, squares and rhombuses for $k_d = 1 \times 10^{-7}$, 2×10^{-7} and 3×10^{-7} m, respectively. Here, R_c stands for the value of R at $t = t_c$. As can be seen, R monotonically decreases with increasing annealing time t. This means that the contribution of the boundary diffusion gradually decreases due to the grain growth in the β layer.

The values of R_c for $k_d = 1 \times 10^{-7}$, 2×10^{-7} and 3×10^{-7} m in Fig. 7 are plotted as open circles, squares and rhombuses, respectively, against the exponent p in Fig. 8. As can be seen, R_c is close to 0.85 at $p = 0.4$ for $k_d = 1 \times 10^{-7}$–3×10^{-7} m, and remains almost constant independently of p for $k_d = 3 \times 10^{-7}$ m. However, for $k_d = 1 \times 10^{-7}$ and 2×10^{-7} m, R_c slightly decreases with increasing value of p. Even in such a case, R_c is still greater than 0.8 at $p = 0.6$. This means that the contribution of the boundary diffusion is more than 80 percent at $t = t_c$. As shown in Fig. 7, the exponent q starts to increase with increasing annealing time at $t = t_c$. However, at $t = t_c$, the contribution of the volume diffusion is less than 20 percent. Consequently, the growth of the β layer is predominantly governed by the boundary diffusion at the plateau stage with $q = q_c$.

The dependence of the exponent q on the ratio R was estimated from the solid and dashed curves in Fig. 7. The results of $k_d = 1 \times 10^{-7}$, 2×10^{-7} and 3×10^{-7} m are shown as solid curves interconnecting open circles, squares and rhombuses, respectively, in Fig. 9. In this figure, the open symbols on the right-hand side show R_c and q_c at $t = t_c$, and those on the left-hand side indicate R and q at $t = 10^7$ s. As can be seen, R_c takes values between 0.80 and 0.85. As the annealing time increases from $t = t_c$ to $t = \infty$ s, the ratio will decrease from $R = R_c$ to $R = 0$, but the exponent should increase from $q = q_c$ to $q = 0.5$. The dependence of q on R considerably varies depending on p, but the solid curves for different values of k_d almost coincide with one another for each value of p. Therefore, the dependence of q on R is predominantly determined by p but not by k_d, though the kinetics of the grain growth is controlled by both k_d and p. The corresponding calculation was carried out also for $D^v = 10^{-16}\,m^2/s$ and $D^b = 10^{-11}\,m^2/s$ at $p = 0.5$. Here, the ratio D^v/D^b is the same as $D^v = 10^{-15}\,m^2/s$ and $D^b = 10^{-10}\,m^2/s$. The results with $k_d = 1 \times 10^{-7}$ and 3×10^{-7} m are shown as solid curves interconnecting open triangles and inverse-triangles, respectively, in Fig. 9. As can be seen, the solid curves with the open triangles and inverse-triangles coincide well with those with the open circles, squares and rhombuses for $p = 0.5$. This means that the dependence of q on R is insensitive to the values of D^v and D^b as long as the ratio D^v/D^b is identical.

The semblable calculation was carried out for various values of D^v at $D^b = 10^{-10}\,m^2/s$, $k_d = 3 \times 10^{-7}$ m and $p = 0.5$. The results for $D^v = 10^{-15}$, 10^{-16} and $10^{-17}\,m^2/s$ are shown as solid curves interconnecting open circles, squares and rhombuses, respectively, in Fig. 10. Also in this figure, the open symbols on the right-hand side indicate R_c and q_c at $t = t_c$, and those on the left-hand side show R and q at $t = 10^7$ s. As D^v decreases from $10^{-15}\,m^2/s$ to $10^{-17}\,m^2/s$, R_c increases from 0.85 to 0.97, but q_c decreases from 0.30 to 0.26. Thus, for $D^v = 10^{-17}\,m^2/s$, a very small value of $q_c = 0.26$ is realized at a large value of $R_c = 0.97$. Consequently, the plateau stage with $q_c = 0.26$ is actualized even at the

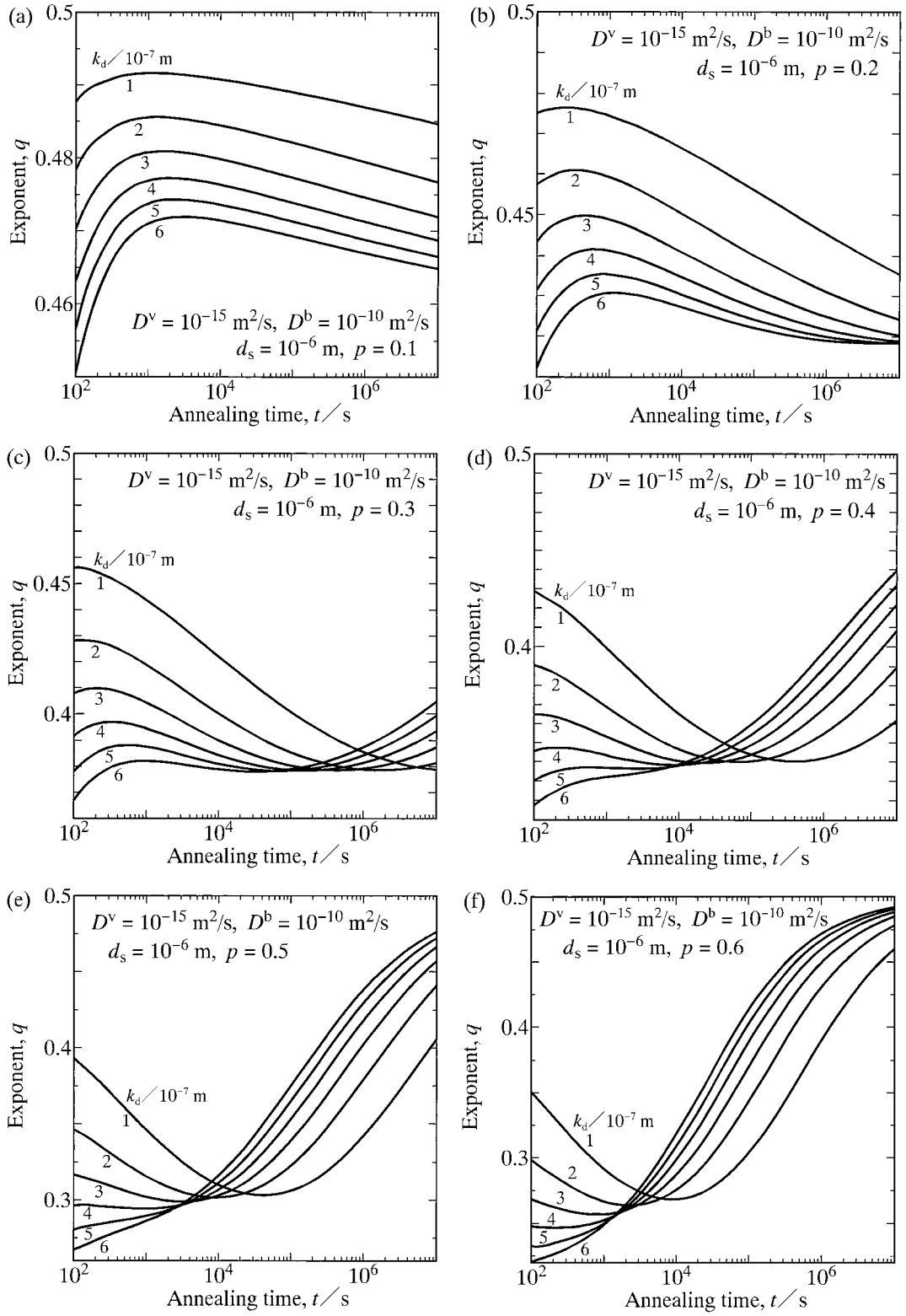

Fig. 5 The exponent q versus the annealing time t calculated for $D^v = 10^{-15}$ m^2/s, $D^b = 10^{-10}$ m^2/s and $k_d = 1 \times 10^{-7}$–6×10^{-7} m at (a) $p = 0.1$, (b) $p = 0.2$, (c) $p = 0.3$, (d) $p = 0.4$, (e) $p = 0.5$ and (f) $p = 0.6$.

annealing time where the contribution of the volume diffusion is merely 3 percent. Considering the curvature, we may expect that the solid curves coincide well with one another at small values of R. As a result, it is concluded that the dependence of q on R varies depending on D^v at large values of R but becomes insensitive to D^v at small values of R.

3.2 Comparison with previous analyses

As mentioned in Sect. 1, the kinetics of the mixed rate-controlling process was theoretically analyzed by Farrell and Glimer.[34] Like the present analysis, they considered a semi-infinite diffusion couple initially consisting of two solid-solution phases with solubility compositions. Thus, there is no diffusional flux in both solid-solution phases. In such a

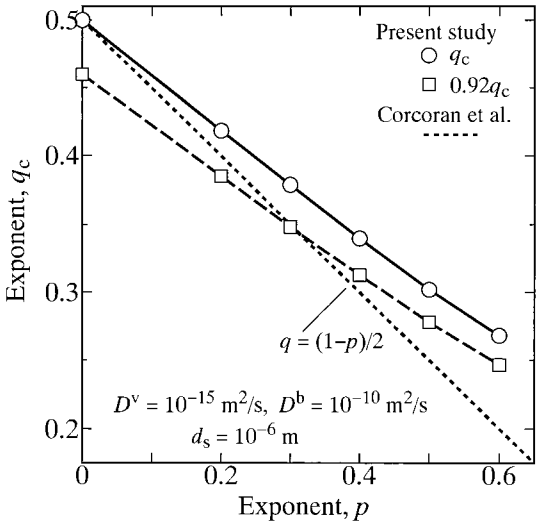

Fig. 6 The exponent q_c versus the exponent p for $D^v = 10^{-15}$ m^2/s and $D^b = 10^{-10}$ m^2/s shown as open circles. Open squares indicate the values smaller by 8 percent than q_c, and a dotted line shows the result deduced from the mathematical model of Corcoran *et al.*[35]

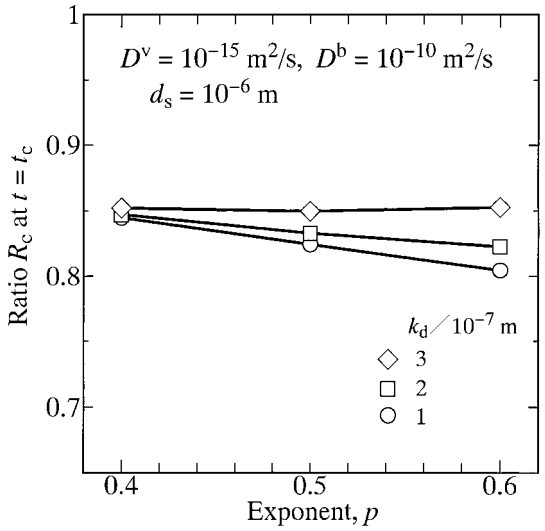

Fig. 8 The ratio R_c at $t = t_c$ versus the exponent p for the results in Fig. 7 with $k_d = 1 \times 10^{-7}$, 2×10^{-7} and 3×10^{-7} m shown as open circles, squares and rhombuses, respectively.

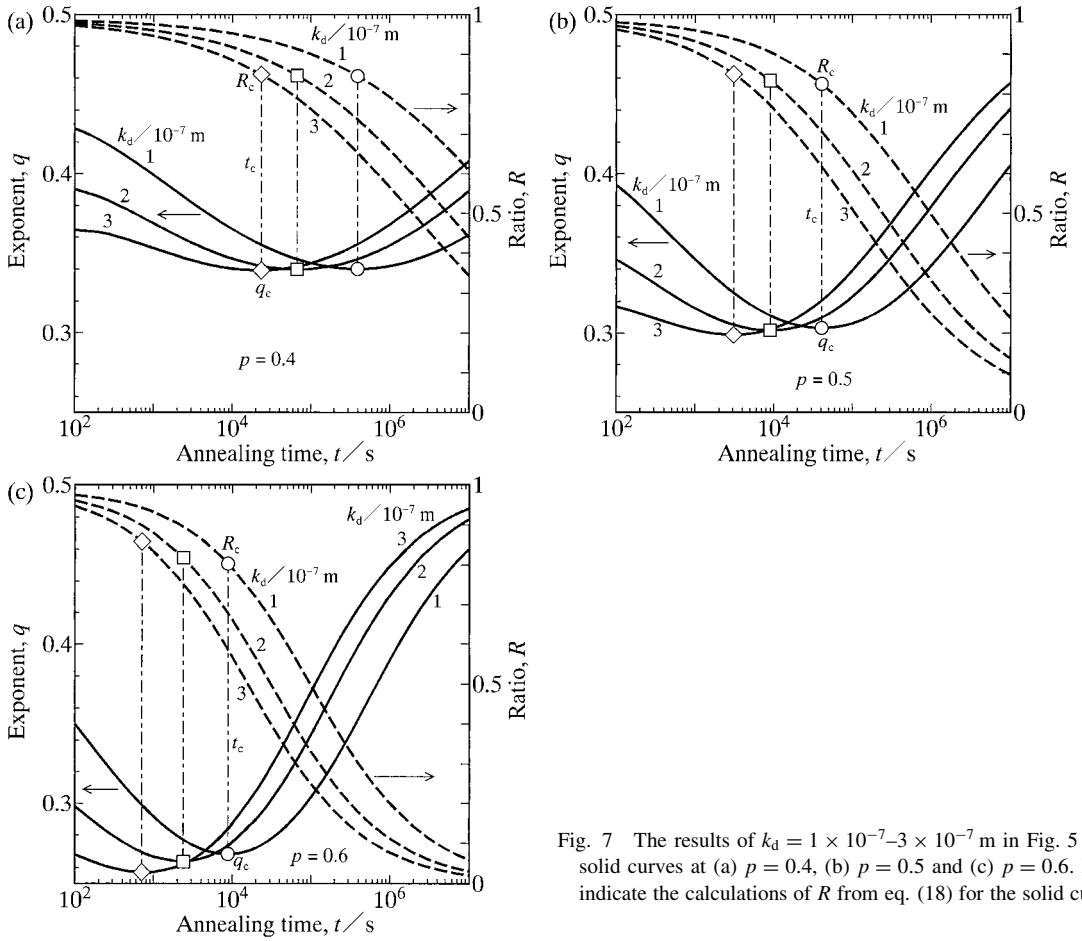

Fig. 7 The results of $k_d = 1 \times 10^{-7}$–3×10^{-7} m in Fig. 5 represented as solid curves at (a) $p = 0.4$, (b) $p = 0.5$ and (c) $p = 0.6$. Dashed curves indicate the calculations of R from eq. (18) for the solid curves.

semi-infinite diffusion couple, a polycrystalline compound layer is formed at the interface between the solid-solution phases. Here, the compound layer with a thickness of z is composed of flat grain boundaries with a thickness of δ and tabular grains, and each tabular grain is sandwiched between two parallel grain boundaries perpendicular to the interface. The distance d between the neighboring parallel grain boundaries is identical for all the tabular grains, and the d axis and the z axis are perpendicular to the grain boundary and the interface, respectively. For such a compound layer, the one-dimensional boundary diffusion along the z axis and the two-dimensional volume diffusion along the d axis and the z axis were calculated numerically. Unlike the present analysis, however, the grain size d remains constant during

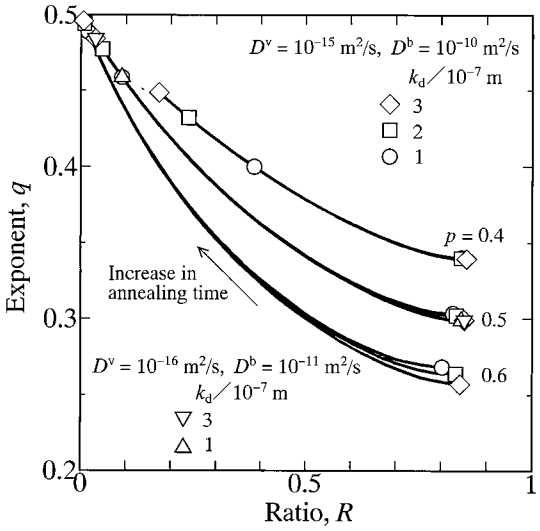

Fig. 9 The exponent q versus the ratio R at annealing times between $t = t_c$ and 10^7 s for the results in Fig. 7 with $k_d = 1 \times 10^{-7}$, 2×10^{-7} and 3×10^{-7} m shown as solid curves interconnecting open circles, squares and rhombuses, respectively. The results for $D^v = 10^{-16}$ m^2/s, $D^b = 10^{-11}$ m^2/s, $p = 0.5$ and $k_d = 1 \times 10^{-7}$ and 3×10^{-7} m are indicated as solid curves interconnecting open triangles and inverse-triangles, respectively.

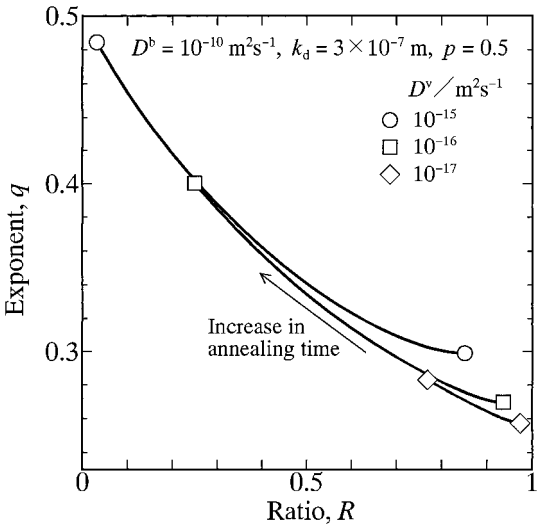

Fig. 10 The exponent q versus the ratio R at annealing times between $t = t_c$ and 10^7 s for $D^b = 10^{-10}$ m^2/s, $p = 0.5$, $k_d = 3 \times 10^{-7}$ m and $D^v = 10^{-15}$, 10^{-16} and 10^{-17} m^2/s shown as solid curves interconnecting open circles, squares and rhombuses, respectively.

growth of the compound layer. This corresponds to the growth with $p = 0$. Their analysis indicates that z is expressed as a power function of t by eq. (16) and q is equal to 0.48. In contrast, the present analysis gives $q = 0.5$ for $p = 0$ as shown in Fig. 4. The discrepancy between $q = 0.48$ and 0.5 is attributed to the volume diffusion along the d axis. In order for the compound layer to grow continuously, solute atoms should be transported by the boundary diffusion along the grain boundary parallel to the z axis over long distances. However, the solute atoms in the grain boundary may be partially wasted by the volume diffusion along the d axis. Such wastage will decelerate the growth of the compound layer. Also in the present analysis, it is possible to consider the volume diffusion along the d axis. However, in the square-rectangular grain, there are double d-axes perpendicular to each other. In such a case, the two-dimensional volume diffusion along the double d-axes as well as the one-dimensional volume diffusion along the z axis has to be calculated numerically. However, an unrealistically long computing time is necessary for such a three-dimensional numerical calculation. Consequently, in the present analysis, the one-dimensional volume diffusion along the z axis was considered, but the two-dimensional volume diffusion along the double d-axes was omitted. Nevertheless, influence of the omission on the kinetics can be estimated from the analysis of Farrell and Glimer.[34] According to their analysis, q is decreased by 4 percent due to the one-dimensional volume diffusion along the single d axis. Consequently, q may be diminished by 8 percent owing to the tow-dimensional volume diffusion along the double d-axes. In Fig. 6, open squares show the values of q_c smaller by 8 percent than those with the open circles. In the present analysis, however, the grain size d monotonically increases with increasing annealing time at $t > t_s$. The penetration depth of the volume diffusion along the d axis relative to the grain size d is smaller for the growing grain than for the non-growing grain. Hence, the diminishment may be smaller than 8 percent at large values of p. Consequently, the open squares provide the lower limit for the estimation of q_c.

On the other hand, as mentioned in Sect. 1, the growth of a compound layer controlled by boundary diffusion was theoretically analyzed by Corcoran *et al.*[35] In their analysis, a compound layer in a semi-infinite diffusion couple consists of cylindrical grains with an identical diameter of d, where the rotation axis of the grain with a length of z is perpendicular to the interface and the diameter d increases in proportion to a power function of the annealing time t with an exponent of p. Thus, the thickness of the compound layer is equal to z. Furthermore, only boundary diffusion occurs in the compound layer, but volume diffusion takes place merely in the neighboring phase ahead of the growing compound layer. If the boundary diffusion predominantly governs the growth of the compound layer, the thickness z is expressed as a power function of the annealing time t with an exponent of q. In such a case, the following relationship holds good between p and q.[35]

$$q = \frac{1 - p}{2} \tag{19}$$

The relationship of eq. (19) is shown as a dotted line in Fig. 6. As can be seen, the slope is steeper for the dotted line than for the dashed and solid curves passing through the open squares and circles, respectively. Nevertheless, at $p = 0.2$–0.4, q is rather close to each other between the dashed curve and the dotted line. Consequently, the relationship between p and q is approximately described by eq. (19) in the range of $p = 0.2$–0.4, even though the two-dimensional volume diffusion along the double d-axes is omitted in eq. (19).

4. Conclusions

The kinetics of the reactive diffusion controlled by boundary and volume diffusion was numerically analyzed

for a hypothetical binary system consisting of one intermetallic compound and two primary solid-solution phases using a mathematical model of a semi-infinite diffusion couple. Here, the diffusion couple is initially composed of the two primary solid-solution phases with solubility compositions. During isothermal annealing at a certain temperature, a layer of the intermetallic compound is formed at the interface in the diffusion couple due to the reactive diffusion between the primary solid-solution phases. However, there is no diffusional flux in the primary solid-solution phases. On the other hand, the compound layer consists of a single layer of square-rectangular grains with an identical dimension, where the side length of the basal-plane and the height are d and z, respectively. The z axis is perpendicular to the interface, and hence the basal-plane is parallel to the interface. Therefore, the thickness of the compound layer is equal to z. For simplification of the analysis, the following assumptions were adopted for the compound layer: (A) there is no grain boundary segregation; (B) volume and boundary diffusion occurs along the z axis; and (C) grain growth starts to occur at a certain annealing time. In order to calculate numerically the growth rate of the compound layer, Crank-Nicolson implicit method[48] was combined with a finite-difference technique.[49] When the grain size d remains constant during growth of the compound layer, the thickness of the compound layer is proportional to a power function of the annealing time t and the exponent q of the power function is equal to 0.5. In contrast, q varies depending on t in complicated manners, if d increases in proportion to a power function of t. Around the critical annealing time t_c, however, q is rather insensitive to t. A constant value of q at $t = t_c$ is denoted by q_c. If the diffusion coefficient is five orders of magnitude greater for the boundary diffusion than for the volume diffusion, q_c takes values of 0.5, 0.42, 0.38, 0.34, 0.30 and 0.27 at $p = 0$, 0.2, 0.3, 0.4, 0.5 and 0.6, respectively. Here, p is the exponent of the power function for the grain growth. Considering the influence of the two-dimensional volume diffusion perpendicular to the grain boundary on the kinetics, we obtain $q_c = 0.46$, 0.39, 0.35, 0.32, 0.28 and 0.25 at $p = 0$, 0.2, 0.3, 0.4, 0.5 and 0.6, respectively. Consequently, at $p = 0.2$–0.4, q_c is approximately expressed as a function of p by the equation $q_c = (1 - p)/2$ deduced from the mathematical model of Corcoran *et al.*[35]

Acknowledgement

The present study was supported by the Iketani Science and Technology Foundation in Japan.

REFERENCES

1) B. Lustman and R. F. Mehl: Trans. Met. Soc. AIME **147** (1942) 369–394.
2) D. Horstmann: Stahl. Eisen. **73** (1953) 659–665.
3) S. Storchheim, J. L. Zambrow and H. H. Hausner: Trans. Met. Soc. AIME **200** (1954) 269–274.
4) L. S. Castleman and L. L. Seigle: Trans. Met. Soc. AIME **209** (1957) 1173–1174.
5) L. S. Castleman and L. L. Seigle: Trans. Met. Soc. AIME **212** (1958) 589–596.
6) N. L. Peterson and R. E. Ogilvie: Trans. Met. Soc. AIME **218** (1960) 439–443.
7) Y. Adda, M. Beyeler, A. Kirianenko and M. F. Mauruce: Mem. Sci. Rev. Met. **58** (1961) 716–724.
8) L. S. Birks and R. E. Seebold: J. Nucl. Mater. **3** (1961) 249–259.
9) R. E. Seebold and L. S. Birks: J. Nucl. Mater. **3** (1961) 260–266.
10) G. V. Kidson and G. D. Miller: J. Nucl. Mater. **12** (1964) 61–69.
11) W. E. Sweeney, Jr. and A. P. Batt: J. Nucl. Mater. **13** (1964) 87–91.
12) K. Shibata, S. Morozumi and S. Koda: J. Japan Inst. Met. **30** (1966) 382–388.
13) K. Hirano and Y. Ipposhi: J. Japan Inst. Met. **32** (1968) 815–821.
14) T. Nishizawa and A. Chiba: J. Japan Inst. Met. **34** (1970) 629–637.
15) M. M. P. Janssen: Metall. Trans. **4** (1973) 1623–1633.
16) G. F. Bastin and G. D. Rieck: Metall. Trans. **5** (1974) 1817–1826.
17) M. Onishi and H. Fujibuchi: Trans. JIM **16** (1975) 539–547.
18) E. I.-B. Hannech and C. R. Hall: Mater. Sci. Tech. **8** (1992) 817–824.
19) P. T. Vianco, P. F. Hlava and A. L. Kilgo: J. Electron. Mater. **23** (1994) 583–594.
20) M. Watanabe, Z. Horita and M. Nemoto: Interface Science **4** (1997) 229–241.
21) S. Choi, T. R. Bieler, J. P. Lucas and K. N. Subramanian: J. Electron. Mater. **28** (1999) 1209–1215.
22) T. Takenaka, M. Kajihara, N. Kurokawa and K. Sakamoto: Mater. Sci. Eng. A **406** (2005) 134–141.
23) Y. Muranishi and M. Kajihara: Mater. Sci. Eng. A **404** (2005) 33–41.
24) T. Hayase and M. Kajihara: Mater. Sci. Eng. A **433** (2006) 83–89.
25) Y. Tanaka, M. Kajihara and Y. Watanabe: Mater. Sci. Eng. A **445–446** (2007) 355–363.
26) D. Naoi and M. Kajihara: Mater. Sci. Eng. A **459** (2007) 375–382.
27) K. Mikami and M. Kajihara: J. Mater. Sci. **42** (2007) 8178–8188.
28) M. Kajihara, T. Yamada, K. Miura, N. Kurokawa and K. Sakamoto: Netsushori **43** (2003) 297–298.
29) T. Yamada, K. Miura, M. Kajihara, N. Kurokawa and K. Sakamoto: J. Mater. Sci. **39** (2004) 2327–2334.
30) T. Yamada, K. Miura, M. Kajihara, N. Kurokawa and K. Sakamoto: Mater. Sci. Eng. A **390** (2005) 118–126.
31) M. Kajihara and T. Takenaka: Mater. Sci. Forum **539–543** (2007) 2473–2478.
32) J. D. Baird: J. Nucl. Energy A **11** (1960) 81–88.
33) F. Brossa, A. Hubaux, D. Quataert and H. W. Schleicher: Mem. Sci. Rev. Metall. **63** (1966) 1–10.
34) H. H. Farrell and G. H. Glimer: J. Appl. Phys. **45** (1974) 4025–4035.
35) Y. L. Corcoran, A. H. King, N. de Lanerolle and B. Kim: J. Electron. Mater. **19** (1990) 1177–1183.
36) K. Suzuki, S. Kano, M. Kajihara, N. Kurokawa and K. Sakamoto: Mater. Trans. **46** (2005) 969–973.
37) M. Mita, M. Kajihara, N. Kurokawa and K. Sakamoto: Mater. Sci. Eng. A **403** (2005) 269–275.
38) T. Takenaka, S. Kano, M. Kajihara, N. Kurokawa and K. Sakamoto: Mater. Sci. Eng. A **396** (2005) 115–123.
39) T. Takenaka, S. Kano, M. Kajihara, N. Kurokawa and K. Sakamoto: Mater. Trans. **46** (2005) 1825–1832.
40) M. Mita, K. Miura, T. Takenaka, M. Kajihara, N. Kurokawa and K. Sakamoto: Mater. Sci. Eng. B **126** (2006) 37–43.
41) T. Takenaka and M. Kajihara: Mater. Trans. **47** (2006) 822–828.
42) T. Takenaka, M. Kajihara, N. Kurokawa and K. Sakamoto: Mater. Sci. Eng. A **427** (2006) 210–222.
43) Y. Yato and M. Kajihara: Mater. Sci. Eng. A **428** (2006) 276–283.
44) Y. Yato and M. Kajihara: Mater. Trans. **47** (2006) 2277–2284.
45) S. Sasaki and M. Kajihara: Mater. Trans. **48** (2007) 2642–2649.
46) W. Jost: Diffusion of Solids, Liquids, Gases (Academic Press, New York, 1960) p. 68.
47) M. Kajihara: Acta Mater. **52** (2004) 1193–1200.
48) J. Crank: The Mathematics of Diffusion (Oxford Univ. Press, London, 1979) p. 144.
49) R. A. Tanzilli and R. W. Heckel: Trans. Met. Soc. AIME **242** (1968) 2313–2321.
50) G. Dahlquist and Å. Björck: Numerical Methods (Prentice-Hall, Englewood Cliffs, NJ, 1974) p. 137.